THE JOURNAL OF PHYSICAL CHEMISTRY B
A JOURNAL OF THE AMERICAN CHEMICAL SOCIETY

pubs.acs.org/JPCB

Article

Tug-of-War between DNA Chelation and Silver Agglomeration in DNA−Silver Cluster Chromophores

Jeffrey T. Petty,*,‡ David Lewis,‡ Savannah Carnahan, Dahye Kim, and Caroline Couch

Cite This: J. Phys. Chem. B 2022, 126, 3822−3830

Read Online

ACCESS | Metrics & More | Article Recommendations | Supporting Information

ABSTRACT: Supramolecular chromophores form when a DNA traps silvers that then coalesce into clusters with discrete, molecular electronic states. However, DNA strands are polymeric ligands that disperse silvers and thus curb agglomeration. We study this competition using two chromophores that share three common components: a dimeric DNA scaffold, Ag^+-nucleobase base pairs, and Ag^0 chromophores. The DNA host C_4-A_2-iC_4T mimics structural elements in a DNA-cluster crystal structure using a phosphodiester backbone with combined 5′ → 3′ and 3′ → 5′ (indicated by "*i*") directions. The backbone directions must alternate to form the two silver clusters, and this interdependence supports a silver-linked structure. This template creates two chromophores with distinct sizes, charges, and hence spectra: $(C_4\text{-}A_2\text{-}iC_4T)_2/Ag_{11}^{7+}$ with $\lambda_{abs}/\lambda_{em}$ = 430/520 nm and $(C_4\text{-}A_2\text{-}iC_4T)_2/Ag_{14}^{8+}$ with $\lambda_{abs}/\lambda_{em}$ = 510/630 nm. The Ag^+ and Ag^0 constituents in these partially oxidized clusters are linked with structural elements in C_4-A_2-iC_4T. Ag^+ alone binds sparsely but strongly to form C_4-A_2-iC_4T/3−4 Ag^+ and $(C_4\text{-}A_2\text{-}iC_4T)_2$/7−8 Ag^+ complexes, and these stoichiometries suggest that Ag^+ cross-links pairs of cytosines to form a hairpin with a metallo-C_4/iC_4 duplex and an adenine loop. The Ag^0 are chemically orthogonal because they can be oxidatively etched without disrupting the underlying Ag^+−DNA matrix, and their reactivity is attributed to their valence electrons and weaker chelation by the adenines. These studies suggest that Ag^+ disperses with the cytosines to create an adenine binding pocket for the Ag^0 cluster chromophores.

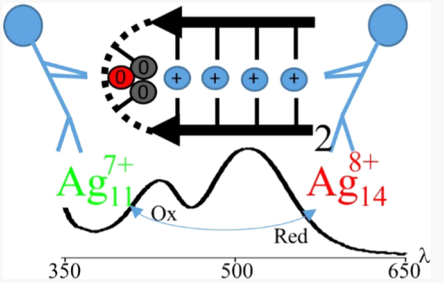

INTRODUCTION

DNA is a robust chemical platform for a range of nanostructures.[1] The base pairs and grooves in duplex DNA sequester organic dyes and precisely regulate the spectra and photophysics of these multichromophore arrays.[2] Stacked base pairs are sets of ligands that chelate and spatially organize metal cations, and these metal-laden strands are potential building blocks for molecular electronic devices.[3−7] Repeated functional groups in a polymeric DNA can be selectively modified and yield peripheral networks of chromophores that efficiently harvest light.[8] In addition to the opportunities afforded by duplex DNA, single-stranded DNA is a template by which hybridization guides and efficiently screens new chemical reactions.[9] Here, we use an oligonucleotide to synthesize molecular silver chromophores.

Single-stranded oligonucleotides are scaffolds for reduced silver clusters because they act as a brake—they coordinate and trap silvers and prevent unrestrained agglomeration that leads to nanoparticles.[10−15] Clusters are synthesized when a DNA locally concentrates Ag^+; then, these DNA-bound Ag^+ are partly reduced and coalesce within the confines of their DNA host (Figure 1A).[10,16−22] The resulting clusters with 6−30 silvers are optical chromophores due to their valence 5s electrons, and they survive precipitation in aqueous buffers and degradation in serum solutions presumably because they are encapsulated and protected by their DNA host.[23−25] These strands have a critical length of 10−20 nucleotides, and four factors control how a polymeric DNA holds its cluster cargo.[26−28] First, DNA sequence sets specific coordination environments. Nucleobases preferentially coordinate silvers but with different affinities, so a particular pattern of nucleobase ligands encodes the cluster spectra.[17,26,27,29−33] Second, DNA structure shapes binding sites. A single-stranded oligonucleotide can both encapsulate a cluster and hybridize with a complement.[16,34−40] Complementary base pairs block cluster binding sites on nucleobases and force a DNA-bound cluster to reorganize, which can enhance emission by $\lesssim 10^3$ fold. Third, a flexible DNA wraps around a cluster to give compact and emissive conjugates because hinge sites allow the oligonucleotide to fold.[41−43] Fourth, DNA strands assemble around a shared cluster. DNA homo- and heterodimers control the fluorescence spectrum and ns kinetics in addition to the slower sub-ms relaxation from long-lived excited states.[31,44−46] Because natural DNA has a 5′ → 3′ direction, dimers can have either an antiparallel, as in the folded lid of a box-like DNA

Received: February 12, 2022
Revised: April 27, 2022
Published: May 20, 2022

https://doi.org/10.1021/acs.jpcb.2c01054
J. Phys. Chem. B 2022, 126, 3822−3830

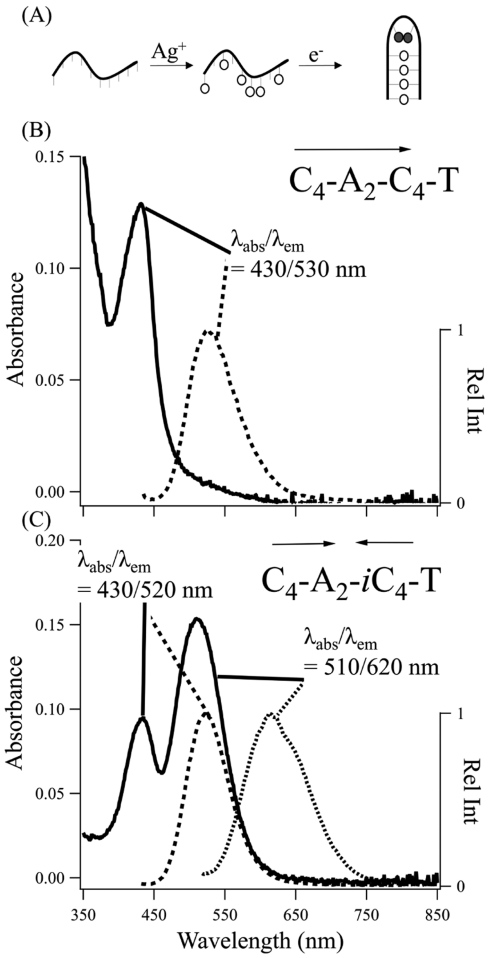

Figure 1. (A) Schematic of synthesis for DNA-bound silver clusters. Open and closed circles represent Ag^+ and Ag^0, respectively. (B, C) Absorption (left axis) and emission (right axis) spectra of the C_4-A_2-C_4T/cluster (B) and C_4-A_2-iC_4T/cluster (C) chromophores. Arrows depict backbone polarity.

construct, or a parallel configuration, which is a focus of our studies.[47−49]

Atomically detailed maps of DNA coordination sites are revealed through crystal structures, and two observations suggest that DNA is a pliable template that can be shaped by silvers. First, DNA is plastic because specific nucleobases contact silvers while others are pushed out of the coordination site.[50,51] Thus, silver adducts reconfigure their polydentate DNA hosts. Second, DNA chelation and silver agglomeration compete, as highlighted in the crystal structure of the green-emitting $(A_2C_4)_2/Ag_8$ complex.[48] The silvers arrange as in the Big Dipper asterism because a handle-like array disperses with the cytosines and a dipper-like subcluster develops with the adenines. Guided by this structure with both dispersed and clustered silvers, we studied how silver clusters with Ag^+ and Ag^0 constituents organize with a DNA host.

Within DNA-bound silver clusters, the Ag^0 garner the most attention because their valence electrons produce strong emission.[10,23,52,53] However, the clusters are partially oxidized, and mass spectra have measured the Ag^+ and Ag^0 constituents for specific chromophores.[21,30,54] Extended X-ray absorption fine structure (EXAFS) and X-ray absorption near-edge structure (XANES) spectra of DNA/Ag_{10}^{6+} complexes reveal distinct scattering paths that were attributed to a Ag^0-rich core within a Ag^+−DNA shell.[55,56] Mass and optical spectra of the green emissive $(C_2A)_6$-Ag_{10}^{6+} complex show that Ag^+ is decoupled from the Ag^0 chromophore.[28] Longer strands such as $(C_2A)_8$ form larger clusters such as Ag_{12}^{8+}, and the added Ag^+ do not disrupt the Ag^0 spectra. Electronic spectra and theoretical calculations indicate that Ag^+ and Ag^0 form small clusters that disperse along DNA templates.[31] We consider how Ag^+ is tied to and shapes distinct parts of a DNA host.

We studied two partially oxidized DNA−silver cluster chromophores using a DNA template with a modified backbone. The phosphodiester linkages of a DNA have a direction or polarity because adjacent deoxyribonucleotides are connected via their respective 5′ and 3′ hydroxyl groups. Besides the natural 5′ → 3′ orientation, the opposite 3′ → 5′ order is achieved with synthetic variants and can be used to create parallel duplexes.[57] Such a duplex is found in the $(A_2C_4)_2/Ag_8$ complex, whose two strands line up side by side to create a cytosine−cytosine duplex and an adenine binding pocket.[48] In the present studies, these two structural elements were mimicked by an oligonucleotide with an adenine bridge between two cytosine tracts, whose backbone linkages were flipped to favor a parallel duplex. This template creates binding sites for two cluster adducts with distinct Ag^+ and Ag^0 constituents. The Ag^+ cross-links cytosines to build a common Ag^+−DNA scaffold that supports the two Ag^0 chromophores. These latter adducts are both optically and chemically distinct, as one can be preferentially etched. We discuss how the DNA, Ag^+, and Ag^0 are organized to understand their spectra and reactivity.

METHODS

Oligonucleotides (Integrated DNA Technologies) were synthesized using the phosphoramidite method, and sequences with inverted polarities switched the positions of the dimethoxytrityl group to protect the 3′ hydroxyl group and the diisopropylamino group as the leaving group on the 5′ hydroxyl group of the deoxyribose.[57] Molar extinction coefficients for the single-stranded oligonucleotides were calculated based on the nearest-neighbor approximation, and the concentrations of these DNA stock solutions were determined using the Lambert−Beer law.[58] The following oligonucleotides were used: CCCCAA*i*C*i*C*i*C*i*CT, CCCCAACCCCT, CCCCAA*i*C*i*C*i*C*i*C, CC*i*C*i*CAACC*i*-C*i*CT, CC*i*C*i*CAA*i*C*i*CCCT, CCCCAA*i*C*i*C*i*C*i*C-teg-CCCCAA*i*C*i*C*i*C*i*CT, GCTCAGCCCTCTTAT-CCCCAA*i*-C*i*C*i*C*i*CT, and CCCCAA*i*C*i*C*i*C*i*C-ATAAGAGGGCT-GAGC, where *i* indicates nucleotides with inverted polarities. The last two strands were designed to form a canonical duplex with C_4-A_2-iC_4 appendages and were slowly annealed in a solution with 60 mM $NaClO_4$.[59]

A typical synthesis used a 150 μL sodium cacodylate buffer (5 mM, pH = 7) with 30 μM C_4-A_2-iC_4T and 120 μM $AgNO_3$ (4 Ag^+/DNA).[42] The mixture was heated to ∼80 °C for 5 min and then cooled with tap water. Prior calorimetry studies measured a Ag^+ affinity of $\sim 6 \times 10^6$ M^{-1} (oligo); so, our conditions of 30 μM DNA and 120 μM Ag^+ suggest ∼93% of the added Ag^+ complexes with the oligonucleotide.[41] An aqueous solution of $NaBH_4$ was added to give a concentration of 120 μM (4 BH_4^-/DNA). The resulting solution was then treated with 400 psi O_2 at 0 °C for 2−3 h in a high-pressure reactor to favor stable, partially oxidized clusters.[60] Clusters were etched with freshly prepared $KMnO_4$ and then purified by dialysis via a 2000 MWCO filter (Vivaspin 20-Sartorius)

https://doi.org/10.1021/acs.jpcb.2c01054
J. Phys. Chem. B 2022, 126, 3822−3830

that retains the DNA−silver complexes and eliminates weakly bound silvers. The resulting samples were supplemented with 1.7 equiv Ag^+ and then exposed to H_2 at 400 psi, which was chosen because it is a weaker reducing agent than BH_4^-.[61]

Absorption spectra were collected on a Cary 50 UV−vis spectrophotometer (Varian), and steady-state emission spectra were collected on a Fluoromax-3 spectrofluorometer (Jobin-Yvon Horiba). Electrospray ionization mass spectrometry (Q-TOF G2-S, Waters) was collected by diluting samples with 2 mM ammonium acetate (pH = 7) to ∼2 μM oligonucleotide and infused at 30 μL/min. The spectra were collected in the negative ion mode with a capillary voltage of −2.7 kV, a sampling cone voltage of −15 V, an extraction cone voltage of 10 V, a cone gas flow of 45 L/h, and a desolvation gas flow of 450 L/h. The source temperature was 80 °C, and the desolvation temperature was 150 °C. Mass calibration was performed using aggregates of sodium formate in the 400 < m/z < 2000 range. The spectra were analyzed using MassLynx V4.1.

RESULTS

Two DNA−silver cluster chromophores were synthesized, and we generally describe how these complexes were dissected to identify their components. The DNA scaffold is distinguished by its phosphodiester backbone with both normal 5′ → 3′ and inverted 3′ → 5′ internucleotide linkages, and the coordination environments were characterized by the optical spectra of their cluster adducts. These clusters are partially oxidized with sizes and charges that were measured by mass spectrometry. Their Ag^+ and Ag^0 constituents were studied from both bottom-up and top-down perspectives. Ag^+ alone forms specific DNA complexes whose Ag^+ and DNA stoichiometries were measured using mass spectrometry. The Ag^0 are chemically labile, and etched clusters were identified via their size and charge using optical and mass spectra.

Reversed Backbone. Two oligonucleotides with identical sequences but different backbones are distinct templates. We considered the phosphodiester backbone because it serially links and orients the nucleobase ligands that coordinate silvers. C_4-A_2-C_4T is a typical oligonucleotide with 5′ → 3′ internucleotide connections, whereas C_4-A_2-iC_4T has the same sequence but its backbone runs 5′ → 3′ for $C_{\underline{1}}$-$A_{\underline{6}}$ and switches to 3′ → 5′ for $iC_{\underline{7}}$-$iC_{\underline{10}}$ using a 3′−3′ internucleotide linkage, where underlined subscripts represent the nucleobase positions in the strand (Figure 1B,C). The $T_{\underline{11}}$ was added because it is more economical to synthesize strands that begin with a normal phosphoramidite. This nucleobase is a weak ligand for silver; so, strands with and without the $T_{\underline{11}}$ form the same two clusters (Figure S1).[27,62] The two strands differ because C_4-A_2-C_4T yields a cluster with λ_{abs} = 430 nm and λ_{em} = 530 nm, while C_4-A_2-iC_4T produces clusters with $\lambda_{abs}/\lambda_{em}$ = 430/520 and 510/610 nm. These spectral signatures were used to probe how the phosphodiester backbone shapes the cluster coordination site.

The backbone and the associated cluster binding sites were further reconfigured by varying the positions, types, and mixtures of internucleotide connections. The 3′−3′ junction was moved to the $C_{\underline{4}}$-$iA_{\underline{5}}$ junction, and this C_4-iA_2-iC_4T mimics the original C_4-A_2-iC_4T with the same two absorptions (Figure S2). Besides a 3′−3′ junction, a 5′−5′ connection also flips the backbone direction, and this junction was inserted between $iC_{\underline{4}}$ and $A_{\underline{5}}$ to give iC_4-A_2-C_4T. Although it is oppositely phased relative to C_4-A_2-iC_4T, this new strand yields the same spectra (Figure S3). Mixed 3′−3′ and 5′−5′ junctions were also combined to further segregate the DNA backbone. C_2-iC_2-A_2-C_2-iC_2T mimics C_4-A_2-iC_4T with two absorptions, while C_2-iC_2-A_2-iC_2-C_2T parallels the normal C_4-A_2-C_4T with one dominant absorption (Figure S4). Thus, the C_4 and C_2 tracts require alternating polarities for the dual absorption/emission, and this interdependence suggests a silver-dependent DNA structure. The silvers that create this structure were counted using mass spectrometry.

Partially Oxidized Silver Molecules. The C_4-A_2-iC_4T/silver cluster chromophores have precise numbers of silvers and DNA strands, and these stoichiometries were measured by electrospray ionization mass spectrometry.[21,63] Oligonucleotides become partially protonated and neutralized during desolvation and develop multiple ions, and C_4-A_2-iC_4T/silver cluster complexes form three sets of ions with overall −4, −5, and −6 charges (Figure 2). These conjugates have two DNA strands that share 11 and 14 silvers, i.e., $(C_4$-A_2-$iC_4T)_2/Ag_{11}$ and $(C_4$-A_2-$iC_4T)_2/Ag_{14}$. These silver clusters are partially oxidized, and their oxidation states were derived from the number of phosphate-bound H^+ in these complexes.

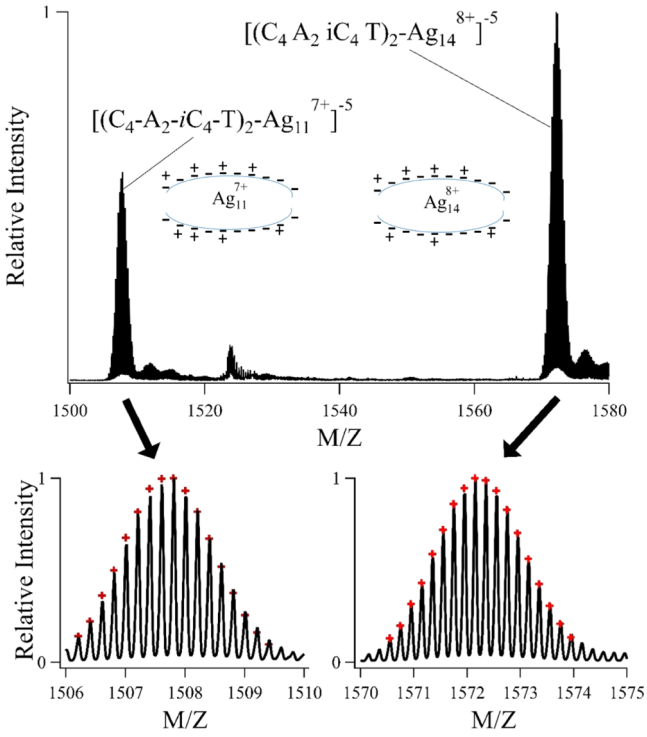

Figure 2. (Top) Mass/charge spectra of $(C_4$-A_2-$iC_4T)_2/Ag_{11}^{7+}$ and $/Ag_{14}^{8+}$ with overall −5 charges. The insets show how the partially oxidized clusters displace H^+ from the DNA backbones of the two C_4-A_2-iC_4T strands to maintain an overall −5 charged ion. (Bottom) Expanded view of the isotopic fine structure with red tick marks that represent the predicted masses based on the following molecular formulas $[C_{204}H_{256}N_{72}O_{126}P_{20}(Ag_{11}^{7+})]^{-5}$ (left) and $[C_{204}H_{255}N_{72}O_{126}P_{20}(Ag_{14}^{8+})]^{-5}$ (right). The precisions between the observed and predicted masses of the isotopologues are 1.0 and 1.7 ppm, respectively.

The complexes are synthesized in an oxygen atmosphere to favor partially oxidized and chemically stable clusters, but Ag^+ adducts change their DNA host.[21,56,60,64] When Ag^+ conjugates with DNA, the host strand maintains its overall charge by

https://doi.org/10.1021/acs.jpcb.2c01054
J. Phys. Chem. B 2022, 126, 3822−3830

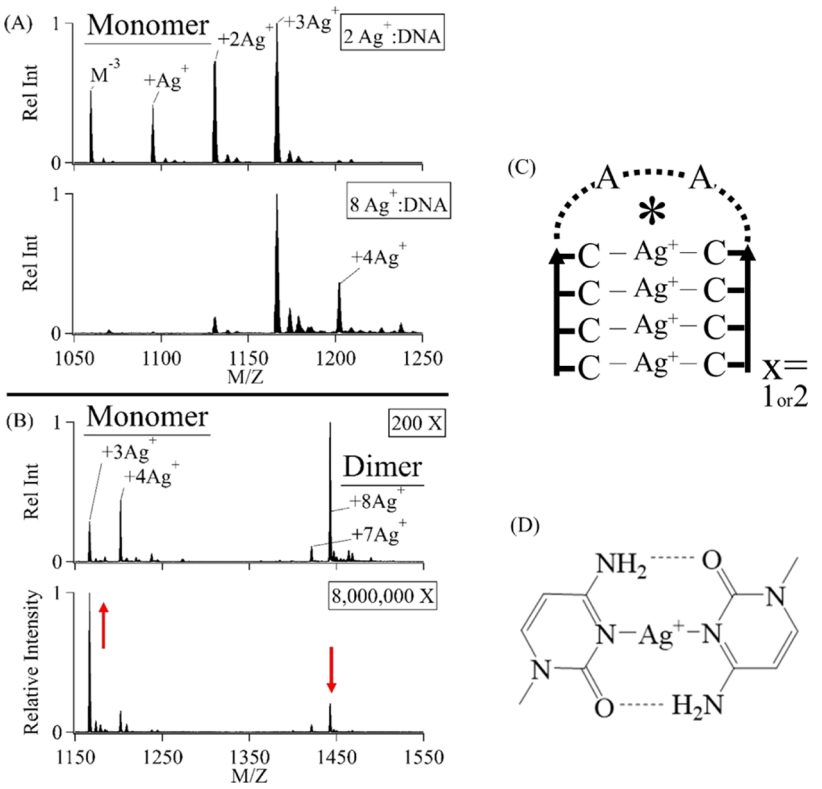

Figure 3. (A) Mass/charge spectra of monomeric C_4-A_2-iC_4T (labeled M) prepared with initial concentrations of 2 Ag^+/DNA and 8 Ag^+/DNA, respectively. The favored complexes are $[C_4\text{-}A_2\text{-}iC_4T/3{-}4\ Ag^+]^{-3}$. (B) Mass/charge spectra of dimeric $[(C_4\text{-}A_2\text{-}iC_4T)_2/7{-}8\ Ag^+]^{-5}$ with dilutions of 200× and 8,000,000×, respectively. Higher dilution shifts the dimeric to monomeric DNA complexes, consistent with the dissociation of an intermolecular complex. (C) Proposed hairpin structure of monomeric and dimeric $[C_4\text{-}A_2\text{-}iC_4T/3{-}4\ Ag^+]$ complexes with 4 cytosine–Ag^+–cytosine base pairs. The * indicates the proposed binding site for the Ag^0. (D) Proposed model for a C–Ag^+–C base pair with N3 chelation of the silvers. The parallel strands allow complementary hydrogen bonding between cytosines.

shedding acidic H^+ from its phosphates, and the number of displaced H^+ matches that of Ag^+, in accordance with XANES spectra.[56] These displaced H^+ are counted using the isotopic fine structure in the mass spectra (Figure 2). A DNA-cluster ion has an envelope of peaks that is prescribed by its molecular formula with its natural distribution of isotopes, and the peak positions and distributions of these isotopologues can be predicted within ±1 H^+ based on our ∼2 ppm m/z precision, and we compared the unligated $(C_4\text{-}A_2\text{-}iC_4T)_2$ dimer with its like-charged DNA-cluster counterparts. For example, the −5 charged $[(C_4\text{-}A_2\text{-}iC_4T)_2]^{-5}$ dimer has the molecular formula $C_{204}H_{\underline{263}}N_{72}O_{126}P_{20}$, whereas the silver-laden $[(C_4\text{-}A_2\text{-}iC_4T)_2/Ag_{11}]^{-5}$ and $[(C_4\text{-}A_2\text{-}iC_4T)_2/Ag_{14}]^{-5}$ counterparts have the respective molecular formulas $C_{204}H_{\underline{256}}N_{72}O_{126}P_{20}Ag_{11}$ and $C_{204}H_{\underline{255}}N_{72}O_{126}P_{20}Ag_{14}$, where the changing number of hydrogens is emphasized by underlining (Figure 2). The latter two formulas with ±1 H^+ do not match the observed distribution (Figure S5).[65] Thus, in relation to the DNA dimer alone, $[(C_4\text{-}A_2\text{-}iC_4T)_2/Ag_{11}]^{-5}$ and $[(C_4\text{-}A_2\text{-}iC_4T)_2/Ag_{14}]^{-5}$ are missing 7 and 8 H^+ because they are displaced by 7 and 8 Ag^+, respectively. This difference is also observed for the −4 and −6 charged ions (Tables S1 and S2). Thus, the Ag_{11}^{7+} and Ag_{14}^{8+} clusters have similar numbers of Ag^+ (7 vs 8, respectively) and different numbers of Ag^0 (4 vs 6, respectively) that yield the dual absorption/emission (Figure 1C). The mass spectra not only identify the number and charge of the silvers but also show that the DNA host is a dimer, and we intentionally linked two strands to recreate the binding sites.

The DNA pair was replicated in solution by preassembling C_4-A_2-iC_4 scaffolds in two ways. First, two C_4-A_2-iC_4 scaffolds were covalently linked with a flexible triethylene glycol (teg).[42] This C_4-A_2-iC_4-teg-C_4-A_2-iC_4T intramolecularly assembles and also produces the λ_{abs} = 430 and 510 nm clusters (Figure S6). Second, C_4-A_2-iC_4 strands were separately appended to the 5′ terminus of one strand and the 3′ terminus of its complement (Figure S7). These studies were based on two well-established characteristics of canonical DNA duplexes. One, duplexes with ≳10 nucleotides are thermally stable, so the appended C_4-A_2-iC_4T strands are pulled together when the duplex anneals. Two, the canonical duplex is antiparallel, so opposite 5′ and 3′ placements of the C_4-A_2-iC_4 appendages precisely position the strands. Like its teg-counterpart, this DNA-forced $(C_4\text{-}A_2\text{-}iC_4)_2$ dimer again yields λ_{abs} = 430 and 510 nm clusters. Thus, in solution, we suggest that an intermolecular $(C_4\text{-}A_2\text{-}iC_4T)_2$ dimer shares Ag_{11}^{7+} and Ag_{14}^{8+} clusters. We next consider how this dimer organizes with its Ag^+ and Ag^0 adducts.

Low Ag^+/DNA Stoichiometries. $(C_4\text{-}A_2\text{-}iC_4T)_2$ forms Ag_{11}^{7+} and Ag_{14}^{8+} clusters that are significantly oxidized, and related complexes form when Ag^+ alone coordinates with C_4-A_2-iC_4T. Ag^+ and DNA were mixed, diluted 40,000× to dissociate weaker adducts, and finally reconcentrated via centrifugal dialysis. These samples produce five sets of ions with overall −2 → −6 charges whose isotope distributions show that the Ag^+ adducts remain fully oxidized (Figure S9D,E). A range of Ag^+ concentrations identify specific Ag^+/DNA complexes (Figures 3A and S8). With an initial concentration of 8 Ag^+/C_4-A_2-iC_4T, most of the added Ag^+

https://doi.org/10.1021/acs.jpcb.2c01054
J. Phys. Chem. B 2022, 126, 3822−3830

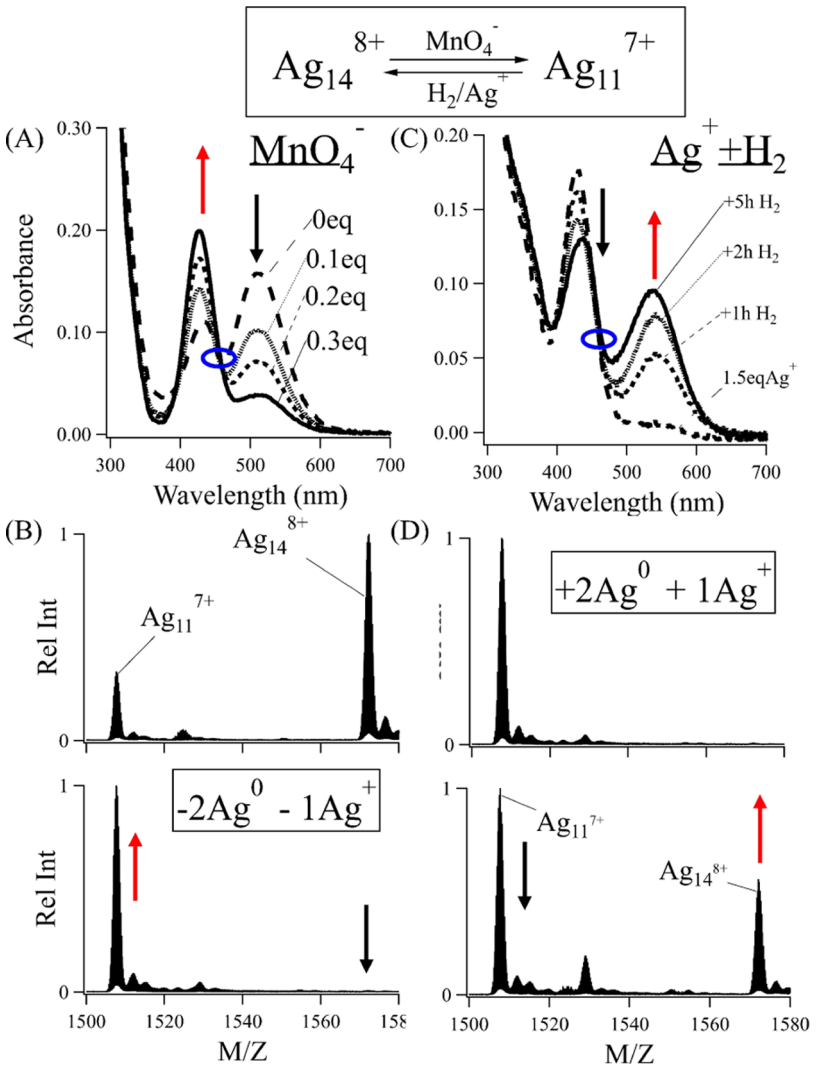

Figure 4. Oxidation and reduction of Ag_{14}^{8+} are reversible. (A/B)MnO_4^- oxidation: (A) absorption spectra show the conversion of λ_{em} = 510 nm to λ_{em} = 430 nm clusters with 0 → 0.3 equiv MnO_4^-. The circled (blue) isosbestic point supports direct conversion between these two clusters. (B) Mass/charge spectra before (top) and after (bottom) adding 0.3 equiv MnO_4^-. The Ag_{14}^{8+} cluster loses 2 Ag^0 and 1 Ag^+. (C, D) H_2 reduction: (C) absorption spectra show the conversion of λ_{em} = 430−510 nm clusters with 0 → 5 h H_2 and 1.5 equiv Ag^+. The circled (blue) isosbestic point supports direct conversion between these two clusters. (D) Mass/charge spectra before (top) and after (bottom) H_2. The Ag_{11}^{7+} cluster gains 2 Ag^0 and 1 Ag^+.

is lost to yield conjugates with only 3−4 Ag^+ (Figure 3A). The stability of these adducts is challenged using less Ag^+. An initial concentration of 4 Ag^+/DNA is only slightly pared down to 3 Ag^+/DNA, while an initial 2 Ag^+/DNA behaves oppositely by climbing up to and favoring 3 Ag^+ (Figure S8). This concentration series shows that dilution effectively eliminates weak adducts to reveal the strongest Ag^+−DNA adducts. Because the polydentate C_4-A_2-iC_4T is rich with nucleobase ligands, the recurring 3−4 Ag^+/DNA stoichiometry suggests that Ag^+ recruits nucleobases to fill its coordination sites (Figure 3C).[18]

Ag^+ also assembles a higher-order dimer $(C_4$-A_2-$iC_4T)_2$/7−8 Ag^+ that is reminiscent of the chromophores (Figures 3B and S9). Relative to the monomeric C_4-A_2-iC_4T/3−4 Ag^+, this dimer has the same empirical stoichiometry and thus may be stabilized by twice the Ag^+−DNA contacts. The stability of the intermolecular dimer was challenged by progressively stronger dilutions from 200× to 40,000× to 8,000,000×. Over this range, the complex tightly secures its 7−8 Ag^+ without shedding individual Ag^+, and only the overall abundance of the $(C_4$-A_2-$iC_4T)_2$/7−8 Ag^+ diminishes. It also forms with a relatively lower starting stoichiometry of 4 Ag^+/DNA (Figure S9F). Thus, this complex cannot be dissected because all 7−8 Ag^+ collectively stabilize this DNA dimer. Because these numbers of Ag^+ are also found in the chromophores, we suggest that a network of Ag^+−DNA contacts anchors and frames the $(C_4$-A_2-$iC_4T)_2/Ag_{11}^{7+}$ and $/Ag_{14}^{8+}$ chromophores.

Ag^0 Etching. With similar numbers of Ag^+, the $(C_4$-A_2-$C_4T)_2/Ag_{11}^{7+}$ vs $(C_4$-A_2-$C_4T)_2/Ag_{14}^{8+}$ chromophores are principally distinguished by their 4 vs 6 Ag^0. These numbers of reduced silvers not only yield distinct spectra but also react differently because MnO_4^- directly converts the 510 nm band to its 430 nm neighbor with an isosbestic point (Figure 4A). Oxidation is supported by two observations. First, the $(C_4$-A_2-$iC_4T)_2/Ag_{11}^{7+}$ and $/Ag_{14}^{8+}$ mixture was combined with MnO_4^- and washed to eliminate byproducts. As result, the Ag_{14}^{8+} is eliminated, and the Ag_{11}^{7+} is preserved, showing that 2 Ag^0 are etched away along with a Ag^+ (Figure 4B). By comparing the

https://doi.org/10.1021/acs.jpcb.2c01054
J. Phys. Chem. B 2022, 126, 3822−3830

optical and mass spectra, the λ_{abs} = 430 and 510 nm chromophores are thus assigned to the Ag_{11}^{7+} and Ag_{14}^{8+} clusters, respectively, and prior studies have identified other Ag_4^0 and Ag_6^0 chromophores with similar spectra.[28,41,42,54] These chromophores have different numbers of Ag^+, again supporting distinct Ag^0 and Ag^+ that comprise the composite clusters. Second, this change is reversed by replenishing the lost silvers (Figures 4C,D and S9). The etched sample with only the λ_{abs} = 430 nm cluster was supplemented with Ag^+, and the reducing agent H_2 recovers the $(C_4\text{-}A_2\text{-}iC_4T)_2/Ag_{14}^{8+}/\lambda_{abs}$ = 510 nm cluster at the expense of its $(C_4\text{-}A_2\text{-}iC_4T)_2/Ag_{11}^{7+}/\lambda_{abs}$ = 430 nm partner (Figures 4C,D and S10). This cycle suggests that MnO_4^- oxidation and H_2 reduction target only the Ag^0 in these complexes. Through these changes, the dimeric DNA and its Ag^+ adducts are conserved.

DISCUSSION

DNA-bound silver clusters balance a competition—multiple nucleobases strongly bind and can disperse silvers, while a subset of silvers agglomerate into molecules with discrete electronic states. These interactions are revealed with atomic details using X-ray diffraction, and our studies were motivated by the $(A_2C_4)_2$ dimer whose cytosine−cytosine duplex forms an elongated silver array and adenine pocket chelates a trapezoidal silver subcluster. These DNA structural elements were integrated into a synthetic template that forms two optically and chemically distinct silver clusters.

Hairpin Structure. C_4-A_2-iC_4T is a polymer with three subunits—C_4 and iC_4 tracts joined by adenines. As a linear chain, the two cytosine tracts are separated, but they are interdependent from a cluster perspective. Their backbones must point in opposite directions to form the λ_{abs} = 430 and 510 nm clusters, and either C_4/iC_4 or iC_4/C_4 order is equivalent. This alternating pattern also holds when the backbone is further segregated into shorter C_2 tracts, and this interdependence is attributed to the DNA structure. The two cytosine tracts could fold to replicate the two structural elements in the $(A_2C_4)_2$ dimer—a parallel cytosine−cytosine duplex with an adenine pocket (Figure 3C). Mass spectra suggest that this DNA hairpin forms because Ag^+ links the C_4 and iC_4 tracts.

Ag^+−DNA Framework. Ag^+ alone binds strongly but sparsely with C_4-A_2-iC_4T to form monomeric and dimeric DNA complexes. Over a wide Ag^+ concentration range, 3−4 Ag^+ sequester with monomeric C_4-A_2-iC_4T, but this is a relatively low concentration given the 11 possible nucleobase ligands. To understand these complexes, the coordination chemistry of Ag^+ with DNA is considered.[18] First, Ag^+ has a stronger affinity for cytosine vs other nucleobases and targets the deprotonated N3 site.[66] Second, it linearly coordinates two cytosines, and the resulting base pairs can stack into thermodynamically stable, extended arrays (Figure 3D).[66−68] Within a flexible C_4-A_2-iC_4T, Ag^+ could cross-link the polydentate C_4 and iC_4 tracts to yield four sets of stacked cytosine−Ag^+ pairs, consistent with our mass spectra (Figure 3C).[4,7] These direct metal−DNA contacts can be further anchored via hydrogen bonds. Within a C_4/iC_4 duplex, the opposing cytosines have inversion symmetry with spatially proximal C2−O and C4−NH_2 groups (Figure 3D).[66,69] The resulting hydrogen bonds would buttress the complex; however, they may be perturbed by their large Ag^+ partner, as suggested by nonplanar and propeller twisted base pairs.[7,48,67,69−72]

Ag^+ also forms dimeric $(C_4\text{-}A_2\text{-}iC_4T)_2/7−8$ Ag^+ complexes with the same empirical stoichiometry as their monomeric C_4-A_2-$iC_4T/3−4$ Ag^+ counterparts, and this twofold difference suggests that the dimer has twice the Ag^+−cytosine base pairs (Figure 3C,D). Prior studies suggest that four-stranded complexes with cytosine sequences can form, so the $(C_4\text{-}A_2\text{-}iC_4T)_2/7−8$ Ag^+ hairpin dimer may be a related structure.[73] With progressively stronger dilutions, these complexes dissociate as a single unit without shedding individual Ag^+ adducts, and this collective stability highlights a strong connection between Ag^+ and DNA.[31,42,44,47,48,51,74] Most importantly, these $(C_4\text{-}A_2\text{-}iC_4T)_2/7−8$ Ag^+ complexes mimic the $(C_4\text{-}A_2\text{-}iC_4T)_2/Ag_{11}^{7+}$ and $/Ag_{14}^{8+}$ chromophores because they both have two DNA strands and 7−8 Ag^+ adducts. Thus, we propose that the Ag^+ in the chromophores are stably bound via Ag^+-cytosine base pairs and thereby form a DNA/Ag^+ framework for these chromophores. Because the favored N3 binding sites on the cytosines are now saturated with Ag^+, we next consider where the Ag^0 locate within their dimeric $(C_4\text{-}A_2\text{-}iC_4T)_2$ host.

Labile Ag^0. After accounting for Ag^+, Ag_{11}^{7+} and Ag_{14}^{8+} have 4 and 6 Ag^0, respectively, and these two clusters not only have distinct spectra but also react differently. Silver molecules can be selectively oxidized because their HOMO−LUMO gaps vary significantly with cluster size.[75] These clusters bound with homopolymers can be etched with appropriate redox partners, and specific DNA-bound clusters can be eliminated via the oxidizing agents O_2 and H_2O_2 to yield more pure solutions of stable complexes.[60,76] Red-emitting silver chromophores are converted to their green counterparts using reactive oxygen species, but these changes can be reversed with BH_4^-.[61,77−79] In our studies, MnO_4^- converts $(C_4\text{-}A_2\text{-}iC_4T)_2/Ag_{14}^{8+}$ with λ_{abs} = 510 nm to $(C_4\text{-}A_2\text{-}iC_4T)_2/Ag_{11}^{7+}$ with λ_{abs} = 430 nm, and isosbestic points in the absorption spectra suggest that this change is direct with no intermediates (Figure 4).[80,81] The etched silvers were removed via dialysis, and then the lost silvers were replenished with Ag^+ and reduced using H_2, a weaker reducing agent than BH_4^-.[61,82] Without replacing the Ag^+, no conversion is observed (Figure S10). Analogously, gold−thiolate nanoclusters can be reductively enlarged but these grow as a snowball by adding both gold and thiol adducts.[80] DNA scaffolds are short polymers, and their finite silver capacity may regulate cluster growth and etching.

The Ag^0 in Ag_{14}^{8+} may react because of not only their valence electrons but also their location. In the C_4-A_2-iC_4T hairpin, Ag^+ saturates the cytosines, and three observations suggest that the Ag^0 are relegated to and loosely restrained in the adenine loop (Figure 3C). First, in relation to cytosine, adenine has a lower affinity for silvers.[17,29] For example, five silvers in the $(A_2C_4)_2/Ag_8$ crystal structure coalesce in the adenine binding pocket, suggesting that silver agglomeration outcompetes DNA chelation.[48] Second, adenine is linked with fluorescence. $(C_2X)_6$ strands produce Ag_{10}^{6+} clusters, which strongly emit only with X = adenines and not X = thymines, imidazoles, and abasic sites.[28] Derivatives of adenine also induce emission. Relative to other nucleobases, X = adenine, 6-methyladenine, 2-aminopurine, and 7-deazaadenine in $C_4XC_4TC_3G$ all yield emissive silver clusters.[32] Third, DNA-bound Ag_{14}^{8+} is pared down using MnO_4^-. When its 2 Ag^0 are oxidized, the resulting Ag^+ do not stay with the DNA but are readily washed away through dialysis. Weakly bound Ag^+ dissociate with dilution, which suggests that the Ag^+ capacity

https://doi.org/10.1021/acs.jpcb.2c01054
J. Phys. Chem. B 2022, 126, 3822−3830

of C_4-A_2-iC_4T has been exceeded. Again, Ag^+ and Ag^0 are distinguished.

CONCLUSIONS

Competing forces can shape supramolecular DNA−silver cluster chromophores. Multiple nucleobases can chelate and disperse silvers, while silvers coalesce and segregate into molecularly sized clusters. We studied how C_4-A_2-iC_4T and its embedded Ag_{11}^{7+} and Ag_{14}^{8+} adducts are organized. This DNA favors these two partially oxidized clusters because its mixed phosphodiester backbone controls how the nucleobases chelate the Ag^+ and Ag^0 constituents. The Ag^+ are active adducts because they migrate to the cytosines to create a stable network of Ag^+−cytosine base pairs. The Ag^0 are more passive adducts because they are relegated to the adenines where they can be oxidatively etched without disrupting the underlying Ag^+−DNA scaffold. This connection between the sequence and structure of a DNA and the organization of its Ag^+/Ag^0 adducts is guiding our efforts to tune the spectra and reactivity of these supramolecular chromophores.

ASSOCIATED CONTENT

Supporting Information

The Supporting Information is available free of charge at https://pubs.acs.org/doi/10.1021/acs.jpcb.2c01054.

Absorption spectra using C_4-A_2-iC_4T vs C_4-A_2-iC_4 templates with and without the terminal thymine, absorption spectra of C_4-A_2-iC_4T vs C_4-iA_2-iC_4T with the 3′−3′ linkage moved to the C_4-iA_5 junction, absorption spectra of C_4-A_2-iC_4T vs iC_4-A_2-C_4T with the relative positions of the C_4 and iC_4 tracts reversed, absorption spectra of C_2-iC_2-A_2-iC_2-C_2-T vs C_2-iC_2-A_2-C_2-iC_2-T with C_2 subtracts, isotopologue distributions with ±1 H^+ with the molecular formula, absorption spectra of the intermolecular $(C_4$-A_2-$iC_4T)_2$ vs the intramolecular C_4-A_2-iC_4-teg-C_4-A_2-iC_4T dimers, absorption spectra of the intermolecular $(C_4$-A_2-$iC_4T)_2$ vs the forced $(C_4$-A_2-$iC_4T)_2$ using the canonical duplex, mass spectra of the C_4-A_2-iC_4T/Ag^+ complexes with 8, 4, and 2 Ag^+/DNA, mass spectra of the $(C_4$-A_2-$iC_4T)_2$/7−8 Ag^+ complexes with 200-, 40,000-, and 8,000,000-fold dilutions and with isotopic distributions to show that the Ag^+ adducts are fully oxidized, and optical spectra of the $(C_4$-A_2-$iC_4T)/Ag_{11}^{7+}$ with Ag^+ and H_2. Two tables describe the observed and predicted m/z differences for the −4, −5, and −6 charged $(C_4$-A_2-$iC_4T)_2/Ag_{11}^{7+}$ and $/Ag_{14}^{8+}$ complexes (PDF)

AUTHOR INFORMATION

Corresponding Author

Jeffrey T. Petty − *Department of Chemistry, Furman University, Greenville, South Carolina 29613, United States;* orcid.org/0000-0003-0149-5335; Email: jeff.petty@furman.edu

Authors

David Lewis − *Department of Chemistry, Furman University, Greenville, South Carolina 29613, United States*

Savannah Carnahan − *Department of Chemistry, Furman University, Greenville, South Carolina 29613, United States*

Dahye Kim − *Department of Chemistry, Furman University, Greenville, South Carolina 29613, United States*

Caroline Couch − *Department of Chemistry, Furman University, Greenville, South Carolina 29613, United States*

Complete contact information is available at: https://pubs.acs.org/10.1021/acs.jpcb.2c01054

Author Contributions

‡J.T.P. and D.L. contributed equally. The manuscript was written through contributions of all authors. All authors have given approval to the final version of the manuscript.

Notes

The authors declare no competing financial interest.

ACKNOWLEDGMENTS

The authors thank the National Science Foundation (CHE-1611451 and CHE-2002910) and the Furman Advantage program. This work was supported, in part, by the National Science Foundation EPSCoR Program under NSF Award No. OIA-1655740. Any opinions, findings, and conclusions or recommendations expressed in this material are those of the author(s) and do not necessarily reflect those of the National Science Foundation.

REFERENCES

(1) Teo, Y. N.; Kool, E. T. DNA-Multichromophore Systems. *Chem. Rev.* **2012**, *112*, 4221−4245.

(2) Armitage, B. A. Cyanine Dye−DNA Interactions: Intercalation, Groove Binding, and Aggregation. In *DNA Binders and Related Subjects*, Waring, M. J.; Chaires, J. B., Eds.; Springer Berlin Heidelberg: Berlin, Heidelberg, 2005; pp 55−76.

(3) Ehrenschwender, T.; Schmucker, W.; Wellner, C.; Augenstein, T.; Carl, P.; Harmer, J.; Breher, F.; Wagenknecht, H. A. Development of a Metal-Ion-Mediated Base Pair for Electron Transfer in DNA. *Chem. - Eur. J.* **2013**, *19*, 12547−12552.

(4) Kondo, J.; Tada, Y.; Dairaku, T.; Hattori, Y.; Saneyoshi, H.; Ono, A.; Tanaka, Y. A Metallo-DNA Nanowire with Uninterrupted One-Dimensional Silver Array. *Nat. Chem.* **2017**, *9*, 956−960.

(5) Hiroyuki, I.; Naomi, Y.; Atsushi, A.; Tomoko, F.; Waka, N.; Shu, S. Electron Mobility in a Mercury-Mediated Duplex of Triazole-Linked DNA (Tldna). *Chem. Lett.* **2011**, *40*, 318−319.

(6) Fardian-Melamed, N.; Katrivas, L.; Eidelshtein, G.; Rotem, D.; Kotlyar, A.; Porath, D. Electronic Level Structure of Silver-Intercalated Cytosine Nanowires. *Nano Lett.* **2020**, *20*, 4505−4511.

(7) Mistry, L.; El-Zubir, O.; Dura, G.; Clegg, W.; Waddell, P. G.; Pope, T.; Hofer, W. A.; Wright, N. G.; Horrocks, B. R.; Houlton, A. Addressing the Properties of "Metallo-DNA" with a Ag(I)-Mediated Supramolecular Duplex. *Chem. Sci.* **2019**, *10*, 3186−3195.

(8) Ensslen, P.; Wagenknecht, H.-A. One-Dimensional Multichromophor Arrays Based on DNA: From Self-Assembly to Light-Harvesting. *Acc. Chem. Res.* **2015**, *48*, 2724−2733.

(9) O'Reilly, R. K.; Turberfield, A. J.; Wilks, T. R. The Evolution of DNA-Templated Synthesis as a Tool for Materials Discovery. *Acc. Chem. Res.* **2017**, *50*, 2496−2509.

(10) Petty, J. T.; Zheng, J.; Hud, N. V.; Dickson, R. M. DNA-Templated Ag Nanocluster Formation. *J. Am. Chem. Soc.* **2004**, *126*, 5207−5212.

(11) Han, B. Y.; Wang, E. K. DNA-Templated Fluorescent Silver Nanoclusters. *Anal. Bioanal. Chem.* **2012**, *402*, 129−138.

(12) Obliosca, J. M.; Liu, C.; Batson, R. A.; Babin, M. C.; Werner, J. H.; Yeh, H.-C. DNA/Rna Detection Using DNA-Templated Few-Atom Silver Nanoclusters. *Biosensors* **2013**, *3*, 185−200.

(13) Petty, J. T.; Story, S. P.; Hsiang, J. C.; Dickson, R. M. DNA-Templated Molecular Silver Fluorophores. *J. Phys. Chem. Lett.* **2013**, *4*, 1148−1155.

(14) Gwinn, E.; Schultz, D.; Copp, S.; Swasey, S. DNA-Protected Silver Clusters for Nanophotonics. *Nanomaterials* **2015**, *5*, 180−207.

(15) Gonzàlez-Rosell, A.; Cerretani, C.; Mastracco, P.; Vosch, T.; Copp, S. M. Structure and Luminescence of DNA-Templated Silver Clusters. *Nanoscale Adv.* **2021**, *3*, 1230−1260.
(16) Yamane, T.; Davidson, N. On the Complexing of Deoxyribonucleic Acid by Silver(I). *Biochim Biophys Acta* **1962**, *55*, 609−621.
(17) Daune, M.; Kekker, C. A.; Schachman, H. K. Complexes of Silver Ion with Natural and Synthetic Polynucleotides. *Biopolymers* **1966**, *4*, 51−76.
(18) Lippert, B.; Sanz Miguel, P. J. The Renaissance of Metal−Pyrimidine Nucleobase Coordination Chemistry. *Acc. Chem. Res.* **2016**, *49*, 1537−1545.
(19) Rabin, I.; Schulze, W.; Ertl, G. Absorption Spectra of Small Silver Clusters Ag_n ($n \geq 3$). *Chem. Phys. Lett.* **1999**, *312*, 394−398.
(20) Schulze, W.; Rabin, I.; Ertl, G. Formation of Light-Emitting Ag_2 and Ag_3 Species in the Course of Condensation of Ag Atoms with Ar. *ChemPhysChem* **2004**, *5*, 403−407.
(21) Koszinowski, K.; Ballweg, K. A Highly Charged Ag_6^{4+} Core in a DNA-Encapsulated Silver Nanocluster. *Chem. - Eur. J.* **2010**, *16*, 3285−3290.
(22) Swasey, S. M.; Copp, S. M.; Nicholson, H. C.; Gorovits, A.; Bogdanov, P.; Gwinn, E. G. High Throughput near Infrared Screening Discovers DNA-Templated Silver Clusters with Peak Fluorescence Beyond 950 nm. *Nanoscale* **2018**, *10*, 19701−19705.
(23) Zheng, J.; Nicovich, P. R.; Dickson, R. M. Highly Fluorescent Noble-Metal Quantum Dots. *Annu. Rev. Phys. Chem.* **2007**, *58*, 409.
(24) Petty, J. T.; Sengupta, B.; Story, S. P.; Degtyareva, N. N. DNA Sensing by Amplifying the Number of near-Infrared Emitting, Oligonucleotide-Encapsulated Silver Clusters. *Anal. Chem.* **2011**, *83*, 5957−5964.
(25) Sharma, J.; Rocha, R. C.; Phipps, M. L.; Yeh, H.-C.; Balatsky, K. A.; Vu, D. M.; Shreve, A. P.; Werner, J. H.; Martinez, J. S. A DNA-Templated Fluorescent Silver Nanocluster with Enhanced Stability. *Nanoscale* **2012**, *4*, 4107−4110.
(26) Richards, C. I.; Choi, S.; Hsiang, J.-C.; Antoku, Y.; Vosch, T.; Bongiorno, A.; Tzeng, Y.-L.; Dickson, R. M. Oligonucleotide-Stabilized Ag Nanocluster Fluorophores. *J. Am. Chem. Soc.* **2008**, *130*, 5038−5039.
(27) Copp, S. M.; Bogdanov, P.; Debord, M.; Singh, A.; Gwinn, E. Base Motif Recognition and Design of DNA Templates for Fluorescent Silver Clusters by Machine Learning. *Adv. Mater.* **2014**, *26*, 5839−5845.
(28) Petty, J. T.; Ganguly, M.; Rankine, I. J.; Baucum, E. J.; Gillan, M. J.; Eddy, L. E.; Léon, J. C.; Müller, J. Repeated and Folded DNA Sequences and Their Modular Ag_{10}^{6+} Cluster. *J. Phys. Chem. C* **2018**, *122*, 4670−4680.
(29) Soto-Verdugo, V.; Metiu, H.; Gwinn, E. The Properties of Small Ag Clusters Bound to DNA Bases. *J. Chem. Phys.* **2010**, *132*, No. 195102.
(30) Schultz, D.; Brinson, R. G.; Sari, N.; Fagan, J. A.; Bergonzo, C.; Lin, N. J.; Dunkers, J. P. Structural Insights into DNA-Stabilized Silver Clusters. *Soft Matter* **2019**, *15*, 4284−4293.
(31) Ramazanov, R. R.; Sych, T. S.; Reveguk, Z. V.; Maksimov, D. A.; Vdovichev, A. A.; Kononov, A. I. Ag−DNA Emitter: Metal Nanorod or Supramolecular Complex? *J. Phys. Chem. Lett.* **2016**, *7*, 3560−3566.
(32) Petty, J. T.; Ganguly, M.; Yunus, A. I.; He, C.; Goodwin, P. M.; Lu, Y.-H.; Dickson, R. M. A DNA-Encapsulated Silver Cluster and the Roles of Its Nucleobase Ligands. *J. Phys. Chem. C* **2018**, *122*, 28382−28392.
(33) Zhang, Y.; He, C.; Petty, J. T.; Kohler, B. Time-Resolved Vibrational Fingerprints for Two Silver Cluster-DNA Fluorophores. *J. Phys. Chem. Lett.* **2020**, *11*, 8958−8963.
(34) Yeh, H. C.; Sharma, J.; Han, J. J.; Martinez, J. S.; Werner, J. H. A DNA–Silver Nanocluster Probe That Fluoresces Upon Hybridization. *Nano Lett* **2010**, *10*, 3106−3110.
(35) Petty, J. T.; Sergev, O. O.; Nicholson, D. A.; Goodwin, P. M.; Giri, B.; McMullan, D. R. A Silver Cluster−DNA Equilibrium. *Anal. Chem.* **2013**, *85*, 9868−9876.
(36) Obliosca, J. M.; Babin, M. C.; Liu, C.; Liu, Y.-L.; Chen, Y.-A.; Batson, R. A.; Ganguly, M.; Petty, J. T.; Yeh, H.-C. A Complementary Palette of Nanocluster Beacons. *ACS Nano* **2014**, *8*, 10150−10160.
(37) Ganguly, M.; Bradsher, C.; Goodwin, P.; Petty, J. T. DNA-Directed Fluorescence Switching of Silver Clusters. *J. Phys. Chem. C* **2015**, *119*, 27829−27837.
(38) Chen, Y.-A.; Vu, H. T.; Liu, Y.-L.; Chen, Y.-I.; Nguyen, T. D.; Kuo, Y.-A.; Hong, S.; Chen, Y.-A.; Carnahan, S.; Petty, J. T.; Yeh, H.-C. Improving Nanocluster Beacon Performance by Blocking the Unlabeled Nc Probes. *Chem. Commun.* **2019**, *55*, 462−465.
(39) Reveguk, Z. V.; Pomogaev, V. A.; Kapitonova, M. A.; Buglak, A. A.; Kononov, A. I. Structure and Formation of Luminescent Centers in Light-up Ag Cluster-Based DNA Probes. *J. Phys. Chem. C* **2021**, *125*, 3542−3552.
(40) Lin, X.; Zou, L.; Lan, W.; Liang, C.; Yin, Y.; Liang, J.; Zhou, Y.; Wang, J. Progress of Metal Nanoclusters in Nucleic Acid Detection. *Dalton Trans.* **2022**, *51*, 27−39.
(41) Petty, J. T.; Sergev, O. O.; Kantor, A. G.; Rankine, I. J.; Ganguly, M.; David, F. D.; Wheeler, S. K.; Wheeler, J. F. Ten-Atom Silver Cluster Signaling and Tempering DNA Hybridization. *Anal. Chem.* **2015**, *87*, 5302−5309.
(42) He, C.; Goodwin, P. M.; Yunus, A. I.; Dickson, R. M.; Petty, J. T. A Split DNA Scaffold for a Green Fluorescent Silver Cluster. *J. Phys. Chem. C* **2019**, *123*, 17588−17597.
(43) Shah, P.; Thulstrup, P. W.; Cho, S. K.; Bjerrum, M. J.; Yang, S. W. DNA−Rna Chimera Indicates the Flexibility of the Backbone Influences the Encapsulation of Fluorescent Agnc Emitters. *Chem. Commun.* **2014**, *50*, 13592−13595.
(44) Petty, J. T.; Giri, B.; Miller, I. C.; Nicholson, D. A.; Sergev, O. O.; Banks, T. M.; Story, S. P. Silver Clusters as Both Chromophoric Reporters and DNA Ligands. *Anal. Chem.* **2013**, *85*, 2183−2190.
(45) Schultz, D.; Gwinn, E. G. Silver Atom and Strand Numbers in Fluorescent and Dark Ag:Dnas. *Chem. Commun.* **2012**, *48*, 5748−5750.
(46) Petty, J. T.; Carnahan, S.; Kim, D.; Lewis, D. Long-Lived Ag_{10}^{6+} Luminescence and a Split DNA Scaffold. *J. Chem. Phys.* **2021**, *154*, No. 244302.
(47) Petty, J. T.; Nicholson, D. A.; Sergev, O. O.; Graham, S. K. Near-Infrared Silver Cluster Optically Signaling Oligonucleotide Hybridization and Assembling Two DNA Hosts. *Anal. Chem.* **2014**, *86*, 9220−9228.
(48) Huard, D. J. E.; Demissie, A.; Kim, D.; Lewis, D.; Dickson, R. M.; Petty, J. T.; Lieberman, R. L. Atomic Structure of a Fluorescent Ag_8 Cluster Templated by a Multistranded DNA Scaffold. *J. Am. Chem. Soc.* **2019**, *141*, 11465−11470.
(49) Wu, Q.; Liu, C.; Cui, C.; Li, L.; Yang, L.; Liu, Y.; Safari Yazd, H.; Xu, S.; Li, X.; Chen, Z.; Tan, W. Plasmon Coupling in DNA-Assembled Silver Nanoclusters. *J. Am. Chem. Soc.* **2021**, *143*, 14573−14580.
(50) Cerretani, C.; Kanazawa, H.; Vosch, T.; Kondo, J. Crystal Structure of a Nir-Emitting DNA-Stabilized Ag_{16} Nanocluster. *Angew. Chem., Int. Ed.* **2019**, *58*, 17153.
(51) Cerretani, C.; Kondo, J.; Vosch, T. Mutation of Position 5 as a Crystal Engineering Tool for a Nir-Emitting DNA-Stabilized Ag16 Nanocluster. *CrystEngComm* **2020**, *22*, 8136−8141.
(52) Kubo, R. Electronic Properties of Metallic Fine Particles. I. *J. Phys. Soc. Japan* **1962**, *17*, 975−986.
(53) Walter, M.; Akola, J.; Lopez-Acevedo, O.; Jadzinsky, P. D.; Calero, G.; Ackerson, C. J.; Whetten, R. L.; Gronbeck, H.; Häkkinen, H. A Unified View of Ligand-Protected Gold Clusters as Superatom Complexes. *Proc. Natl. Acad. Sci. U.S.A.* **2008**, *105*, 9157−9162.
(54) Copp, S. M.; Schultz, D.; Swasey, S.; Pavlovich, J.; Debord, M.; Chiu, A.; Olsson, K.; Gwinn, E. Magic Numbers in DNA-Stabilized Fluorescent Silver Clusters Lead to Magic Colors. *J. Phys. Chem. Lett.* **2014**, *5*, 959−963.
(55) Petty, J. T.; Ganguly, M.; Rankine, I. J.; Chevrier, D. M.; Zhang, P. A DNA-Encapsulated and Fluorescent Ag_{10}^{6+} Cluster with a Distinct Metal-Like Core. *J. Phys. Chem. C* **2017**, *121*, 14936−14945.

https://doi.org/10.1021/acs.jpcb.2c01054
J. Phys. Chem. B 2022, 126, 3822−3830

(56) Petty, J. T.; Sergev, O. O.; Ganguly, M.; Rankine, I. J.; Chevrier, D. M.; Zhang, P. A Segregated, Partially Oxidized, and Compact Ag_{10} Cluster within an Encapsulating DNA Host. *J. Am. Chem. Soc.* **2016**, *138*, 3469−3477.
(57) Sande, J. H. vd.; Ramsing, N. B.; Germann, M. W.; Elhorst, W.; Kalisch, B. W.; Kitzing, Ev.; Pon, R. T.; Clegg, R. C.; Jovin, T. M. Parallel Stranded DNA. *Science* **1988**, *241*, 551−557.
(58) Bloomfield, V. A.; Crothers, D. M.; Tinoco, I., Jr. *Nucleic Acids: Structures, Properties, and Functions*, University Science Books: Sausaltio, CA, 2000; Chapter 14, p 794.
(59) Markham, N. R.; Zuker, M. Dinamelt Web Server for Nucleic Acid Melting Prediction. *Nucleic Acids Res.* **2005**, *33*, W577−W581.
(60) Petty, J. T.; Story, S. P.; Juarez, S.; Votto, S. S.; Herbst, A. G.; Degtyareva, N. N.; Sengupta, B. Optical Sensing by Transforming Chromophoric Silver Clusters in DNA Nanoreactors. *Anal. Chem.* **2012**, *84*, 356−364.
(61) Cerretani, C.; Vosch, T. Switchable Dual-Emissive DNA-Stabilized Silver Nanoclusters. *ACS Omega* **2019**, *4*, 7895−7902.
(62) Sengupta, B.; Ritchie, C. M.; Buckman, J. G.; Johnsen, K. R.; Goodwin, P. M.; Petty, J. T. Base-Directed Formation of Fluorescent Silver Clusters. *J. Phys. Chem. C* **2008**, *112*, 18776−18782.
(63) Beck, J. L.; Colgrave, M. L.; Ralph, S. F.; Sheil, M. M. Electrospray Ionization Mass Spectrometry of Oligonucleotide Complexes with Drugs, Metals, and Proteins. *Mass Spectrom. Rev.* **2001**, *20*, 61−87.
(64) Schultz, D.; Gardner, K.; Oemrawsingh, S. S. R.; Markeševic′, N.; Olsson, K.; Debord, M.; Bouwmeester, D.; Gwinn, E. Evidence for Rod-Shaped DNA-Stabilized Silver Nanocluster Emitters. *Adv. Mater.* **2013**, *25*, 2797−2803.
(65) Kilgour, D. P. A.; Van Orden, S. L.; Tran, B. Q.; Goo, Y. A.; Goodlett, D. R. Producing Isotopic Distribution Models for Fully Apodized Absorption Mode FT-MS. *Anal. Chem.* **2015**, *87*, 5797−5801.
(66) Tanaka, Y.; Kondo, J.; Sychrovsky, V.; Sebera, J.; Dairaku, T.; Saneyoshi, H.; Urata, H.; Torigoe, H.; Ono, A. Structures, Physicochemical Properties, and Applications of T-Hg^{II}-T, C-Ag^{i}-C, and Other Metallo-Base-Pairs. *Chem. Commun.* **2015**, *51*, 17343−17360.
(67) Terrón, A.; Moreno-Vachiano, B.; Bauzá, A.; García-Raso, A.; Fiol, J. J.; Barceló-Oliver, M.; Molins, E.; Frontera, A. X-Ray Crystal Structure of a Metalled Double-Helix Generated by Infinite and Consecutive C*-AgI-C* (C*:N1-Hexylcytosine) Base Pairs through Argentophilic and Hydrogen Bond Interactions. *Chem. - Eur. J.* **2017**, *23*, 2103−2108.
(68) Terron, A.; Tomas, L.; Bauza, A.; Garcia-Raso, A.; Fiol, J. J.; Molins, E.; Frontera, A. The First X-Ray Structure of a Silver-Nucleotide Complex: Interaction of Ion Ag(I) with Cytidine-5′-Monophosphate. *CrystEngComm* **2017**, *19*, 5830−5834.
(69) Megger, D. A.; Fonseca Guerra, C.; Bickelhaupt, F. M.; Müller, J. Silver(I)-Mediated Hoogsteen-Type Base Pairs. *J. Inorg. Biochem.* **2011**, *105*, 1398−1404.
(70) Ono, T.; Yoshida, K.; Saotome, Y.; Sakabe, R.; Okamoto, I.; Ono, A. Synthesis of Covalently Linked Parallel and Antiparallel DNA Duplexes Containing the Metal-Mediated Base Pairs T−Hg(II)−T and C−Ag(I)−C. *Chem. Commun.* **2011**, *47*, 1542−1544.
(71) Berger, I.; Kang, C.; Fredian, A.; Ratliff, R.; Moyzis, R.; Rich, A. Extension of the Four-Stranded Intercalated Cytosine Motif by Adenine•Adenine Base Pairing in the Crystal Structure of d-(CCCAAT). *Nat. Struct. Biol.* **1995**, *2*, No. 416.
(72) Fortino, M.; Marino, T.; Russo, N. Theoretical Study of Silver-Ion-Mediated Base Pairs: The Case of C−Ag−C and C−Ag−A Systems. *J. Phys. Chem. A* **2015**, *119*, 5153−5157.
(73) Day, H. A.; Huguin, C.; Waller, Z. A. E. Silver Cations Fold I-Motif at Neutral pH. *Chem. Commun.* **2013**, *49*, 7696−7698.
(74) Shah, P.; Nagda, R.; Jung, I. L.; Bhang, Y. J.; Jeon, S.-W.; Lee, C. S.; Do, C.; Nam, K.; Kim, Y. M.; Park, S.; Roh, Y. H.; Thulstrup, P. W.; Bjerrum, M. J.; Kim, T.-H.; Yang, S. W. Noncanonical Head-to-Head Hairpin DNA Dimerization Is Essential for the Synthesis of Orange Emissive Silver Nanoclusters. *ACS Nano* **2020**, *14*, 8697−8706.
(75) Henglein, A.; Mulvaney, P.; Linnert, T. Chemistry of Agn Aggregates in Aqueous-Solution - Nonmetallic Oligomeric Clusters and Metallic Particles. *Faraday Discuss.* **1991**, 31−44.
(76) Linnert, T.; Mulvaney, P.; Henglein, A.; Weller, H. Long-Lived Nonmetallic Silver Clusters in Aqueous Solution: Preparation and Photolysis. *J. Am. Chem. Soc.* **1990**, *112*, 4657−4664.
(77) Choi, S.; Park, S.; Lee, K.; Yu, J. Oxidant-Resistant Imaging and Ratiometric Luminescence Detection by Selective Oxidation of Silver Nanodots. *Chem. Commun.* **2013**, *49*, 10908−10910.
(78) Li, J.; Yu, J.; Huang, Y.; Zhao, H.; Tian, L. Highly Stable and Multiemissive Silver Nanoclusters Synthesized in Situ in a DNA Hydrogel and Their Application for Hydroxyl Radical Sensing. *ACS Appl. Mater. Interfaces* **2018**, *10*, 26075−26083.
(79) Anand, U.; Ghosh, S.; Mukherjee, S. Toggling between Blue- and Red-Emitting Fluorescent Silver Nanoclusters. *J. Phys. Chem. Lett.* **2012**, *3*, 3605−3609.
(80) Yao, Q.; Yuan, X.; Fung, V.; Yu, Y.; Leong, D. T.; Jiang, D.-e.; Xie, J. Understanding Seed-Mediated Growth of Gold Nanoclusters at Molecular Level. *Nat. Commun.* **2017**, *8*, No. 927.
(81) Jin, S.; Wang, S.; Xiong, L.; Zhou, M.; Chen, S.; Du, W.; Xia, A.; Pei, Y.; Zhu, M. Two Electron Reduction: From Quantum Dots to Metal Nanoclusters. *Chem. Mater.* **2016**, *28*, 7905−7911.
(82) Evanoff, D. D.; Chumanov, G. Size-Controlled Synthesis of Nanoparticles. 1. "Silver-Only" Aqueous Suspensions Via Hydrogen Reduction. *J. Phys. Chem. B* **2004**, *108*, 13948−13956.

https://doi.org/10.1021/acs.jpcb.2c01054
J. Phys. Chem. B 2022, 126, 3822−3830

A Tug-of-War between DNA Chelation and Silver Agglomeration in DNA-Silver Cluster Chromophores

Jeffrey T. Petty* †, David Lewis †, Savannah Carnahan, Dahye Kim, and Caroline Couch

Department of Chemistry
Furman University
Greenville, SC 29613

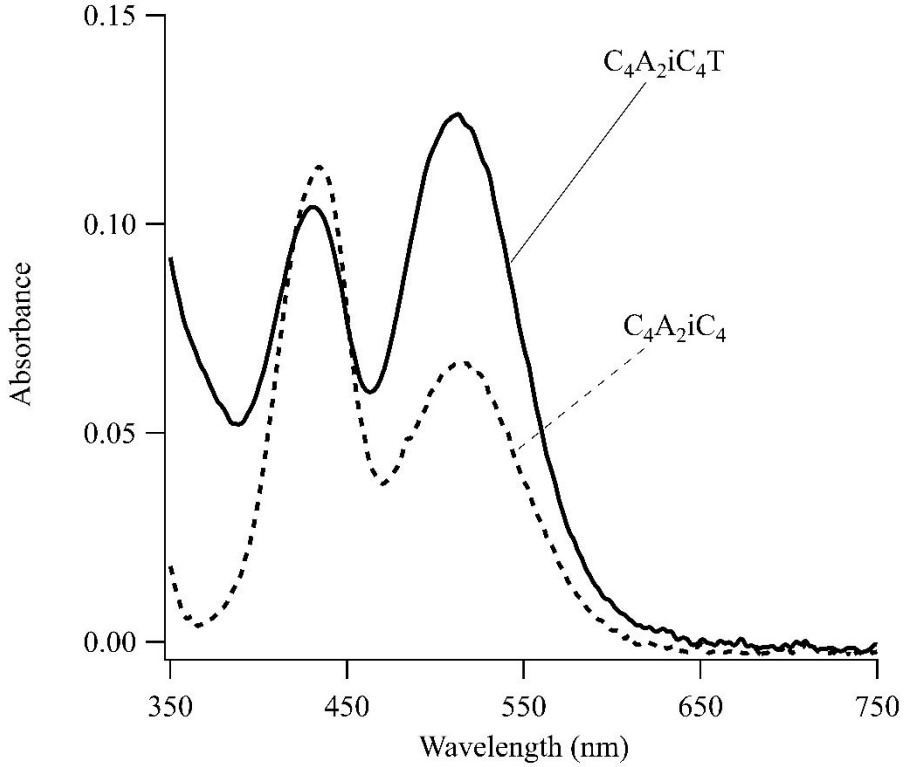

Figure S1: Absorption spectra of C_4-A_2-*i*C_4T (solid) and C_4-A_2-*i*C_4 (dashed) show that 3' terminal thymine preserves the cluster binding sites for both the λ_{abs} = 430 and 510 nm clusters.

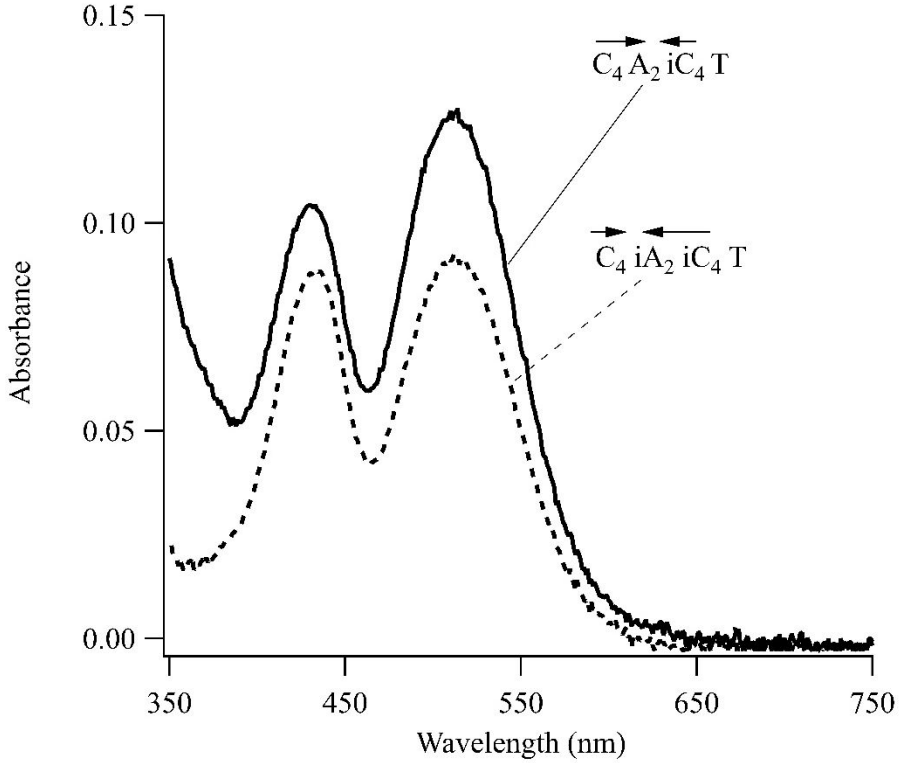

Figure S2: Absorption spectra of C_4-A_2-*i*C_4T (solid) and C_4-*i*A_2-*i*C_4T (dashed) show that the position of the 3'-3' linkage is does not alter the coordination site for the two clusters. Polarities are indicated with arrows above the sequences.

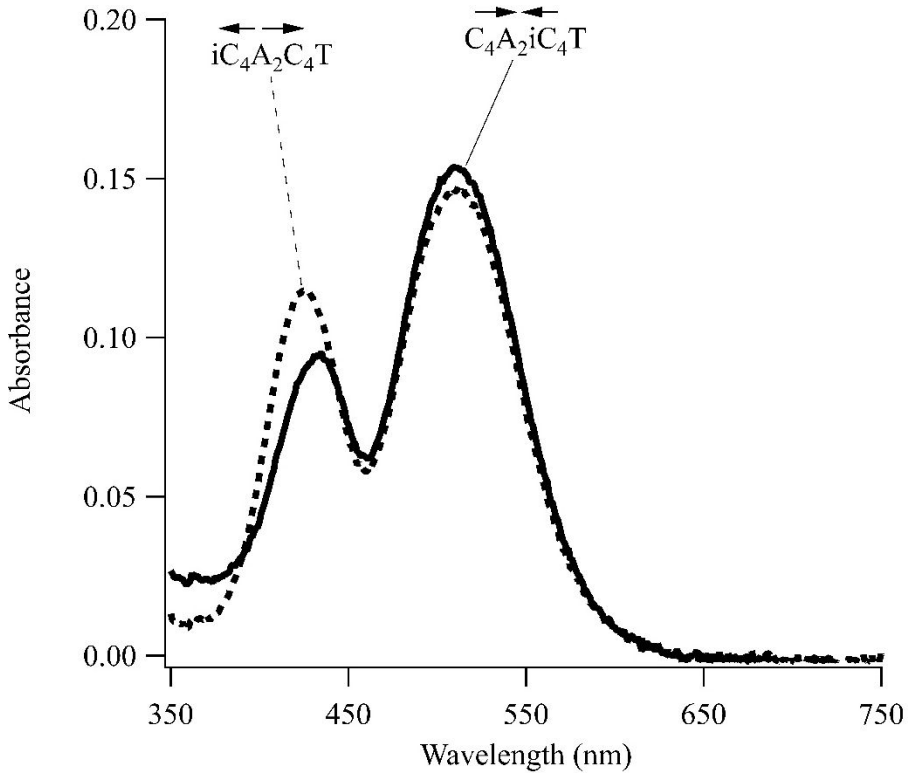

Figure S3: Absorption spectra of C_4-A_2-iC_4T (solid) and iC_4-A_2-C_4T (dashed) show that the position of 3'-3' and 5'-5' linkages, respectively, both yield the same coordination sites for the two clusters. Polarities are indicated with arrows above the sequences.

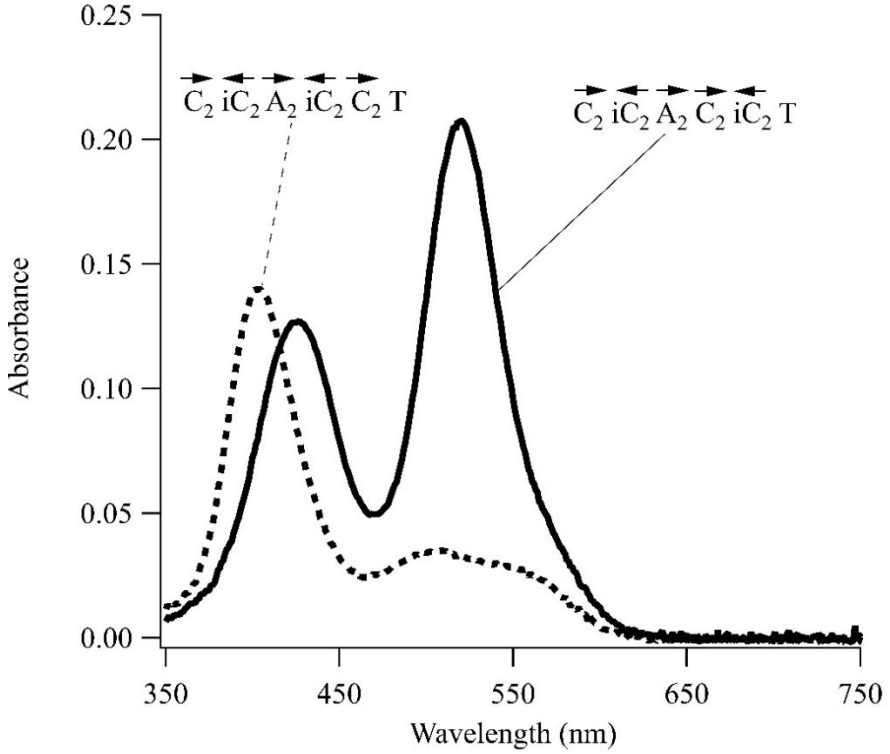

Figure S4: Absorption spectra of C_2-iC_2-A_2-C_2-iC_2T (solid) and C_2-iC_2-A_2-iC_2-C_2T (dashed) show that alternating backbone polarities yield the two clusters. Polarities are indicated with arrows above the sequences.

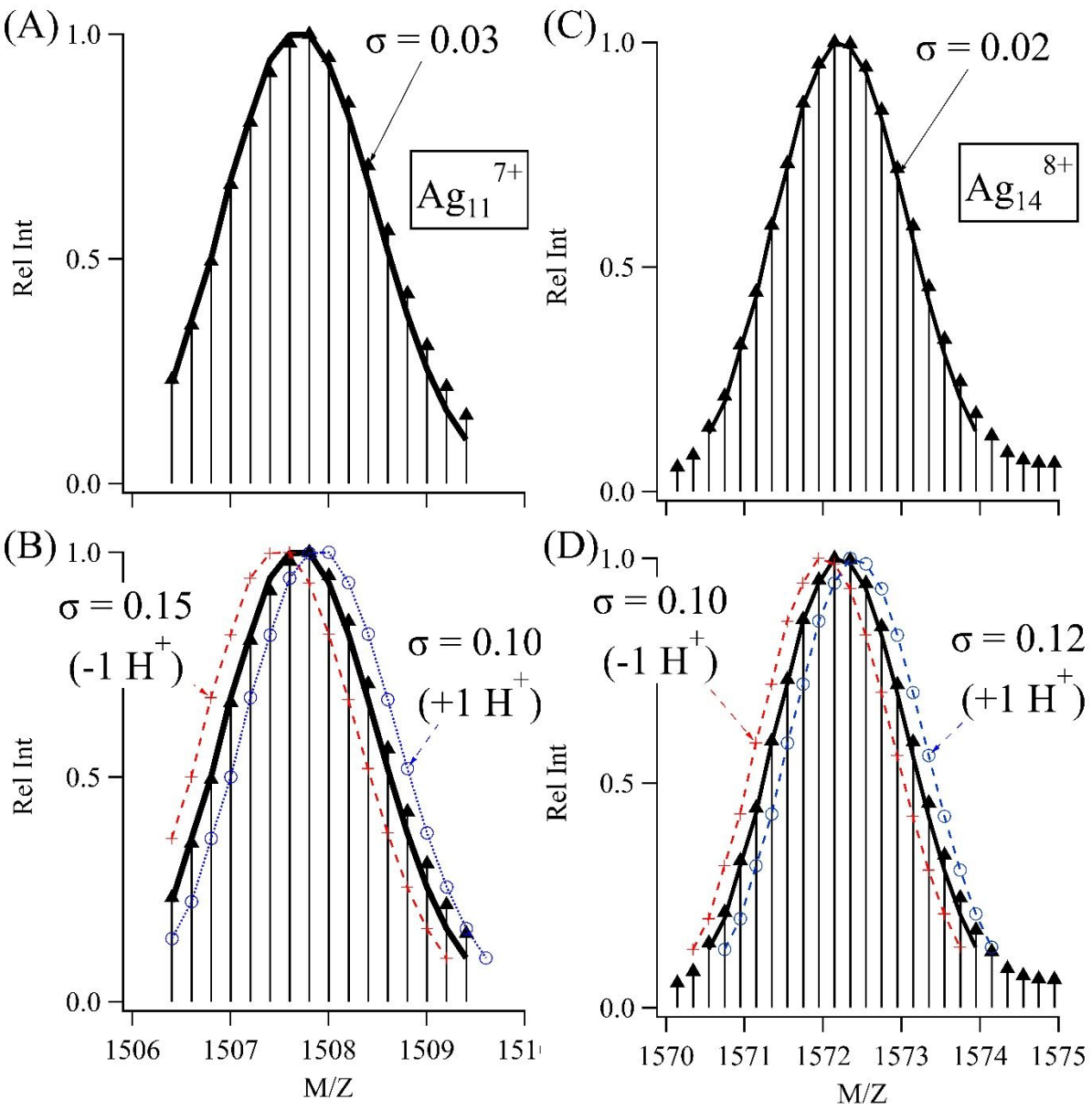

Figure S5: Isotopologue distributions for the -5 charged state based on the molecular formula $[C_{204}H_{256}N_{72}O_{126}P_{20}(Ag_{11}^{7+})]^{-5}$ for $(C_4\text{-}A_2\text{-}iC_4T)_2/Ag_{11}^{7+}$ (A/B) and $[C_{204}H_{255}N_{72}O_{126}P_{20}(Ag_{14}^{8+})]^{-5}$ for $(C_4\text{-}A_2\text{-}iC_4T)_2/Ag_{11}^{7+}$ (C/D). The predicted peaks are indicated by triangles and the standard deviation for the intensity distribution (σ) is based on

$$\sigma = \sqrt{\frac{\Sigma_N (I_{measured} - I_{model})^2}{N-1}}$$

where $I_{measured}$ is the measured intensity, I_{model} is the predicted intensity, and N is the number of peaks in the distribution. Standard deviations with -1 H^+ (red crosses and dotted line) and +1 H^+ (blue circles and dotted line) are larger.

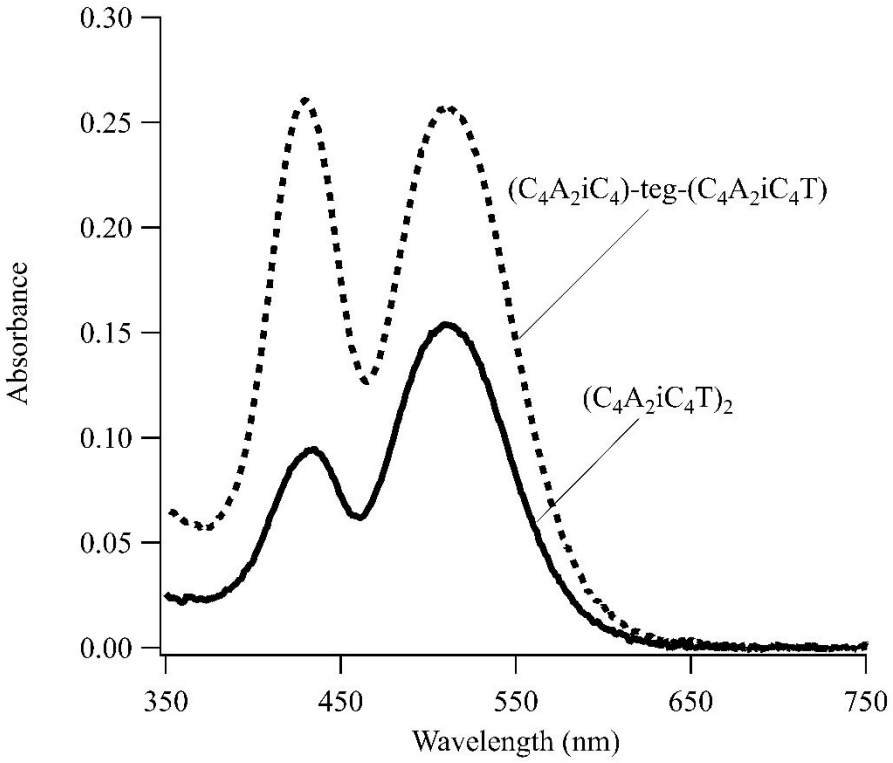

Figure S6: Absorption spectra of C_4-A_2-*i*C_4T (solid) and C_4-A_2-*i*C_4-teg- C_4-A_2-*i*C_4T (dashed) show that preassembling two C_4-A_2-*i*C_4 scaffolds also yields the two clusters.

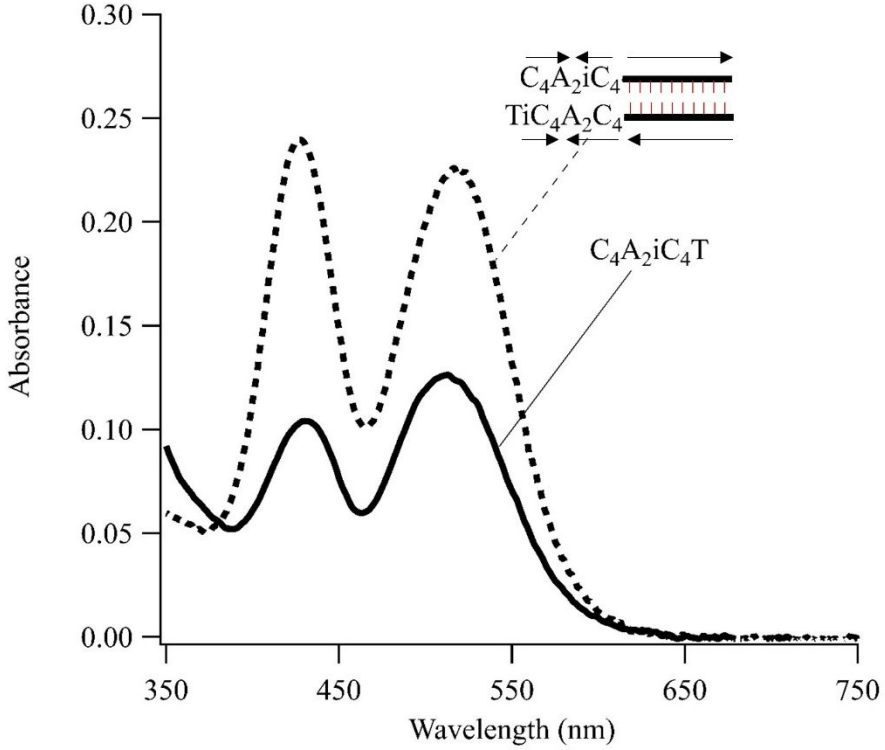

Figure S7: Absorption spectra of C_4-A_2-*i*C_4T (solid) and (C_4-A_2-*i*C_4)$_2$-Duplex (dashed) show that preassembling two C_4-A_2-*i*C_4 scaffolds with parallel C_4/C_4 tracts also yields the two clusters.

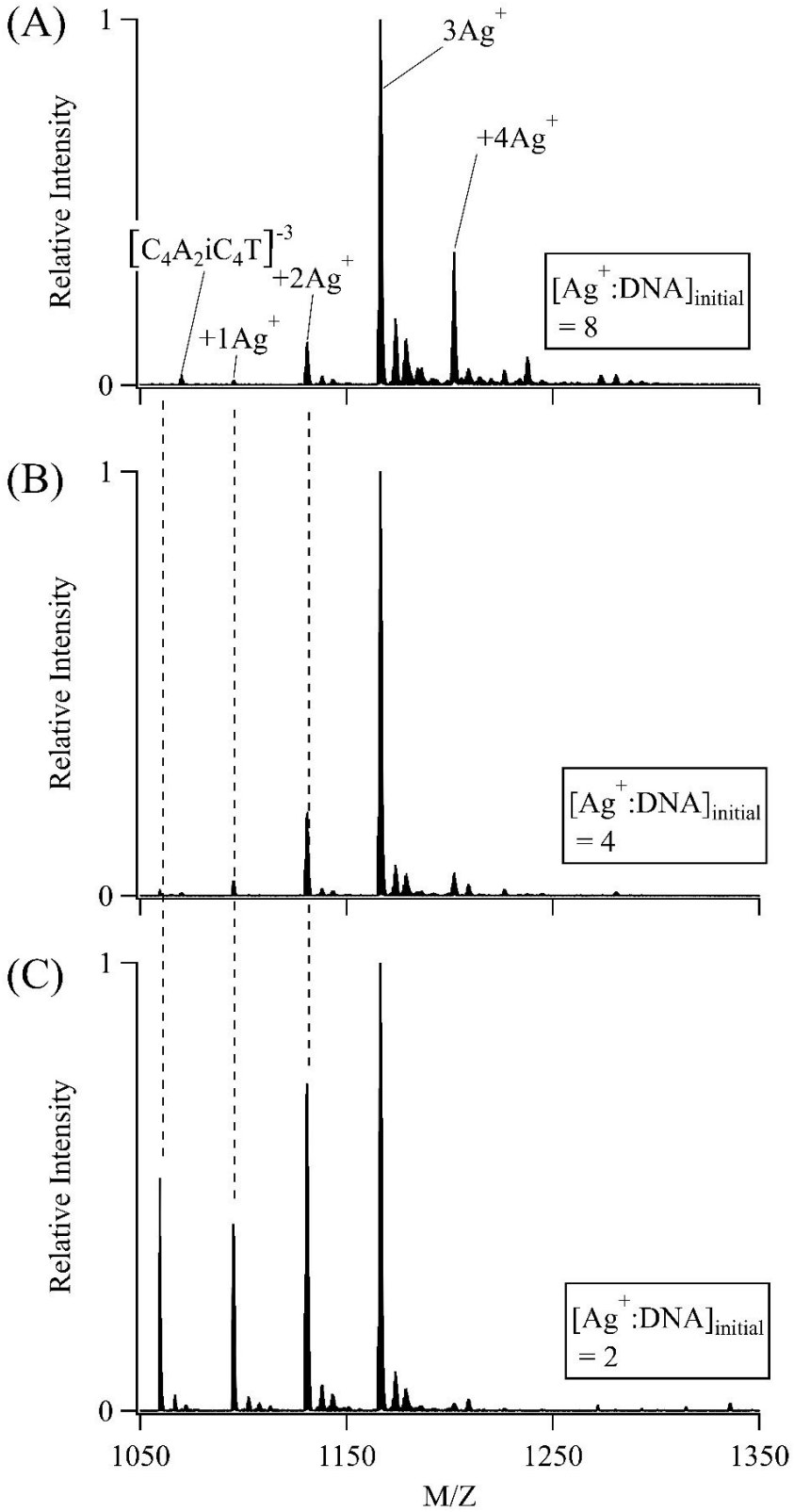

Figure S8: Mass:charge spectra of C_4-A_2-iC_4T prepared with 8, 4, and 2 Ag^+ (A-C, respectively). This range shows that C_4-A_2-iC_4T/3-4 Ag^+ is a favored stoichiometry.

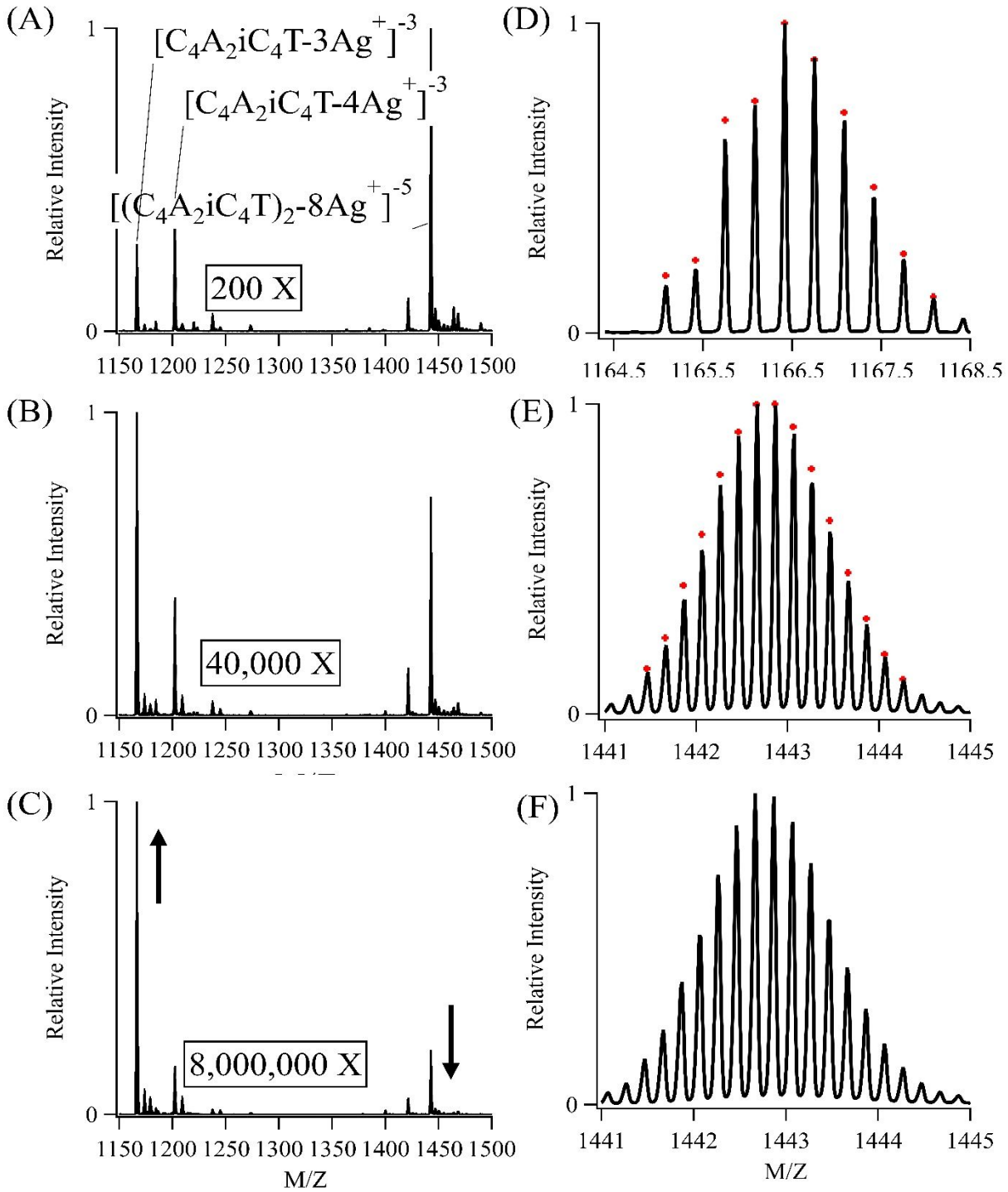

Figure S9: Mass:charge spectra of C_4-A_2-iC_4T prepared with 8 and diluted 200X, 40 000X, and 8 000 000X (A-C, respectively). This range shows that the dimeric $(C_4\text{-}A_2\text{-}iC_4T)_2$/7-8$Ag^+$ dissociates at higher dilution, consistent with an intermolecular complex. (D) Fine-structure mass spectra of the C_4-A_2-iC_4T/3Ag^+ complex. The formula $(C_{102}H_{128}N_{36}O_{63}P_{10}Ag_3)^{-3}$ is missing 3 H^+, showing that the silvers are fully oxidized. . (E) Fine-structure mass spectra of the $(C_4\text{-}A_2\text{-}iC_4T)_2$/8$Ag^+$ complex. The formula $(C_{204}H_{255}N_{72}O_{126}P_{20}Ag_8)^{-5}$ is missing 8 H^+, showing that the silvers are fully oxidized. (F) The $(C_4\text{-}A_2\text{-}iC_4T)_2$/8$Ag^+$ complex is also observed with a starting stoichiometry of 4 Ag^+:DNA.

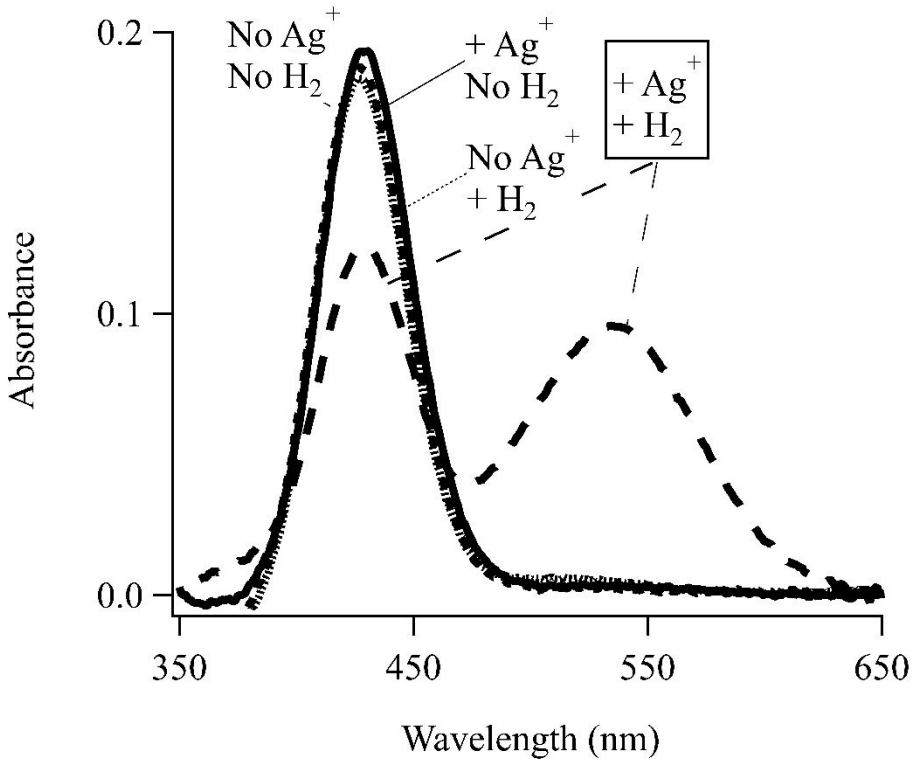

Figure S10: Absorption spectra of C_4-A_2-*i*C_4T/Ag_{11}^{7+} shows that C_4-A_2-*i*C_4T /Ag_{14}^{8+} only forms when both Ag^+ and H_2 are used.

Table S1: Summary of differences between observed and predicted M/Z values (Δ) for the [(C_4-A_2-*i*C_4T)$_2$-Ag_{11}^{7+}]$^{-4}$, [(C_4-A_2-*i*C_4T)$_2$-Ag_{11}^{7+}]$^{-5}$, and [(C_4-A_2-*i*C_4T)$_2$-Ag_{11}^{7+}]$^{-6}$ complexes.[a]

[(C_4-A_2-*i*C_4T)$_2$-Ag_{11}^{7+}]$^{-4}$	Δ(ppm)	[(C_4-A_2-*i*C_4T)$_2$-Ag_{11}^{7+}]$^{-5}$	Δ	[(C_4-A_2-*i*C_4T)$_2$-Ag_{11}^{7+}]$^{-6}$	Δ
1883.004	1.5	1506.204	0.1	1255.003	1.2
1883.255	1.0	1506.405	0.7	1255.170	1.4
1883.506	0.3	1506.606	1.3	1255.333	1.8
1883.756	0.6	1506.806	1.3	1255.502	0.1
1884.007	0.2	1507.006	1.3	1255.667	1.3
1884.257	0.2	1507.206	1.2	1255.835	0.2
1884.507	0.2	1507.406	1.2	1256.002	0.1
1884.757	0.1	1507.606	1.4	1256.169	0.1
1885.008	0.2	1507.806	1.1	1256.335	0.4
1885.258	0.2	1508.006	1.1	1256.502	0.1
1885.508	0.4	1508.206	1.3	1256.669	0.2
1885.757	0.3	1508.406	1.2	1256.835	0.5
1886.008	0.1	1508.607	1.6	1257.003	0.4
1886.258	0.0	1508.807	1.2	1257.169	0.2
1886.507	0.4	1509.006	0.6	1257.336	0.4
1886.759	0.3	1509.205	0.0	1257.503	0.4
1887.006	1.3	1509.407	1.2	1257.669	0.5

[a] Average Δ = 0.7 ppm

Table S2: Summary of differences between observed and predicted M/Z values (D) for the $[(C_4\text{-}A_2\text{-}iC_4T)_2\text{-}Ag_{14}^{8+}]^{-4}$, $[(C_4\text{-}A_2\text{-}iC_4T)_2\text{-}Ag_{14}^{8+}]^{-5}$, and $[(C_4\text{-}A_2\text{-}iC_4T)_2\text{-}Ag_{14}^{8+}]^{-6}$ complexes.[a]

$[(C_4\text{-}A_2\text{-}iC_4T)_2\text{-}Ag_{14}^{8+}]^{-4}$	Δ	$[(C_4\text{-}A_2\text{-}iC_4T)_2\text{-}Ag_{14}^{8+}]^{-5}$	Δ	$[(C_4\text{-}A_2\text{-}iC_4T)_2\text{-}Ag_{14}^{8+}]^{-6}$	Δ
1963.433	0.0	1570.546	0.8	1308.622	1.7
1963.683	0.4	1570.748	1.5	1308.781	4.0
1963.933	0.3	1570.948	1.7	1308.958	3.8
1964.182	0.6	1571.148	1.5	1309.118	1.2
1964.434	0.1	1571.347	1.3	1309.286	0.8
1964.683	0.4	1571.548	1.6	1309.456	1.9
1964.933	0.4	1571.748	1.6	1309.620	0.2
1965.184	0.2	1571.948	1.5	1309.787	0.3
1965.434	0.3	1572.148	1.5	1309.955	1.5
1965.684	0.1	1572.348	1.4	1310.121	0.3
1965.934	0.1	1572.549	1.8	1310.288	0.6
1966.184	0.2	1572.749	1.7	1310.456	2.2
1966.435	0.2	1572.948	1.6	1310.621	0.3
1966.686	0.6	1573.149	2.1	1310.788	0.4
1966.935	0.4	1573.349	2.1	1310.958	3.3
1967.185	0.3	1573.550	2.3	1311.122	0.8
1967.437	1.1	1573.750	2.2	1311.286	1.4
1967.687	1.2	1573.950	2.3	1311.468	10.9

[a]Average Δ = 1.4 ppm